

Extremum Seeking Based on Atmospheric Turbulence for Aircraft Endurance

James P. Krieger* and Miroslav Krstic†
 University of California, San Diego, La Jolla, California 92093-0411

DOI: 10.2514/1.53825

Traditional extremum seeking depends on adding a perturbation to the control input, but it is untenable to continuously perturb the throttle in a controller meant to minimize fuel consumption. Inspired by a recent application of extremum seeking to a fusion reactor where internal nonperiodic perturbations were employed in the seeking process, a novel variant of extremum seeking is proposed that uses naturally occurring stochastic disturbances in lieu of the traditionally added perturbation signal. Relying on airspeed perturbations from atmospheric turbulence to reveal the local slope of the drag curve, the scheme induces a gradient descent to the minimum drag speed. Using stochastic averaging, it is proven analytically that the extremum-seeking controller stabilizes airspeed to the minimum drag speed, with an average offset proportional to the third derivative of the drag curve and the variance of the airspeed. Brief simulation results illustrate the performance of the algorithm.

Nomenclature

A	= aspect ratio
a	= stochastic disturbance post-saturation scaling factor
B	= timescale-shifted and scaled Brownian motion
b	= engine thrust proportionality constant
C_D	= coefficient of drag
C_{Di}	= induced drag coefficient
C_{D0}	= zero-lift drag coefficient
C_L	= coefficient of lift
C_2, C_4	= averaging constants
D	= drag
\bar{D}	= recentered drag function
e	= Oswald efficiency number (also base of natural logarithm)
g	= acceleration due to gravity
J	= Jacobian of a system
k_{ES}	= extremum-seeking gain
k_i	= integral gain
k_p	= proportional gain
L	= lift
L_u, L_v, L_w	= characteristic lengths of turbulence field (longitudinal, lateral, vertical)
m	= mass of the aircraft
n_0, n_1, n_2	= coefficients of the assumed form of $v_{eq}^{e,a}$
q	= stochastic disturbance presaturation scaling factor
S	= reference area
t	= time
U_0	= nominal airspeed for turbulence model
u	= throttle position
V	= airspeed
v	= ground speed
v_*	= minimum drag speed
\hat{v}_*	= estimate of minimum drag speed
W	= standard Brownian motion
ϵ	= turbulence time constant

η	= wind speed, presaturation
$\mu(d\eta)$	= invariant distribution of η
ρ	= air density
σ	= integrator value
$\sigma_u, \sigma_v, \sigma_w$	= root-mean-square turbulence intensity (longitudinal, lateral, and vertical components)
τ_H	= simulation high-pass-filter time constant
τ_L	= simulation low-pass-filter time constant
$\Phi_{u_g}, \Phi_{v_g}, \Phi_{w_g}$	= turbulence spectra (longitudinal, lateral, vertical)
χ	= timescale-shifted wind speed
Ω	= spatial frequency
ω	= temporal frequency

Subscript

eq = equilibrium value

Superscripts

a = average system variable
 e = error variable

Introduction

EXTREMUM seeking is traditionally performed by adding a perturbation signal to the setpoint of a system. The perturbation signal is usually a sinusoid [1–3] but can also be nonsinusoidal [4] or stochastic [5,6]. It is also possible to use naturally occurring disturbances in lieu of an added perturbation signal [7]. Here, this approach is taken to optimize the speed of an aircraft for maximum endurance: that is, to maximize the length of time an aircraft can stay aloft. Convergence to the optimum speed is proven analytically and shown in simulation.

Over the past decade, extremum seeking has been adapted to many different applications, including antilock braking [8], particle beam matching [9], axial compressors [10], lean premixed combustion [11,12], flow control [13], bioreactors [14], tokamak fusion devices [15], and formation flight [16]. Extremum seeking may also be applied to an aircraft optimizing airspeed for best possible endurance. Aircraft wings have an optimal angle of attack that provides a maximum lift-to-drag ratio. All other factors being equal, a jet aircraft flying at the speed that achieves this angle of attack burns fuel more slowly than when flying either slower or faster than this optimal speed. This optimal speed is calculated during the design of the aircraft based on wind-tunnel data; however, the optimal speed for any particular aircraft varies from the calculated value to some degree. The optimal speed varies based on many factors, from

Received 27 January 2011; revision received 29 April 2011; accepted for publication 1 May 2011. Copyright © 2011 by James Krieger and Miroslav Krstic. Published by the American Institute of Aeronautics and Astronautics, Inc., with permission. Copies of this paper may be made for personal or internal use, on condition that the copier pay the \$10.00 per-copy fee to the Copyright Clearance Center, Inc., 222 Rosewood Drive, Danvers, MA 01923; include the code 0731-5090/11 and \$10.00 in correspondence with the CCC.

*Graduate Student, Department of Mechanical and Aerospace Engineering, 9500 Gilman Drive, Mail Code 0411; jkrieger@ucsd.edu.

†Professor, Department of Mechanical and Aerospace Engineering, 9500 Gilman Drive, Mail Code 0411; krstic@ucsd.edu.

manufacturing differences to the condition of the wing. Accumulated bugs, nicks and dents can all change the optimal angle of attack, which changes the airspeed for optimal endurance. Extremum seeking may be used to find the optimal airspeed for the current condition of each individual aircraft as it flies. A recent survey of extremum seeking is given in [17].

While traditional, perturbation-based extremum seeking is a possibility, there are potential disadvantages to using this technique. The first is the possibility that the act of introducing the airspeed perturbation would decrease endurance. Periodically changing the commanded airspeed would cause the throttle command to oscillate, which quite possibly would use more fuel than a more steady throttle command. While finding the optimal airspeed would decrease drag and improve endurance, an oscillating throttle command could use more fuel and hurt endurance.

The second disadvantage to using traditional extremum seeking has less to do with technical performance than aviation administration. It may be seen as undesirable for the speed of an aircraft to be continuously varying. Traditional extremum seeking alters the observable motion of the aircraft, which may act as an impediment to its implementation. Used herein is a form of extremum seeking that relies on naturally occurring disturbances, rather than manually added perturbations, to avoid these disadvantages.

Aircraft in flight on occasion encounter turbulence, which acts as a stochastic disturbance in airspeed. By taking advantage of this, a turbulence-based extremum-seeking algorithm can avoid the disadvantages of traditional extremum seeking. If the throttle is used to control airspeed in response to turbulence, no objection is raised; it is expected that airspeed will be controlled. Doing so does not use any additional fuel. The second disadvantage can be answered similarly; since the aircraft's speed is only being perturbed by turbulence, the observable motion of the aircraft is not altered. These two reasons may make turbulence-based extremum seeking a good fit for this application.

It should be mentioned that steady level flight is not necessarily optimal, but is the only form of flight considered in this paper. Periodic flight consisting of alternating higher-speed climbs and lower-speed glides can achieve endurance superior to steady flight [18–21]. Since such periodic flight would alter the observable motion of the aircraft even more than traditional extremum seeking, only the case of steady flight at a given altitude is considered.

This paper is organized as follows. First, the relevant aerodynamics are reviewed. Next, the dynamic aircraft model is developed and the extremum-seeking control law is designed. An analysis of the stability of the system is then presented, followed by simulation results. A discussion is given and then lastly, some concluding remarks.

Aerodynamics

This section presents the simplified aerodynamic model that is used in the following analysis. Additional background can be found in [22]. Readers comfortable with aerodynamics and turbulence modeling may proceed to the control design below, noting that for simplicity the vertical component of turbulence is ignored.

Lift and Drag

Lift is a function of air density, airspeed, a coefficient of lift, and a reference area. The expression for lift is

$$L = C_L \frac{1}{2} \rho V^2 S \quad (1)$$

The coefficient of lift is a function of angle of attack, and is roughly linear for small angles. Drag is calculated similarly, only using a drag coefficient C_D . Drag is calculated as

$$D = C_D \frac{1}{2} \rho V^2 S \quad (2)$$

The coefficient of drag is commonly calculated as the sum of two parts: the zero-lift drag coefficient and the induced drag coefficient:

$$C_D = C_{D0} + C_{Di} \quad (3)$$

Induced drag is commonly approximated as having a quadratic dependence on the coefficient of lift [23]:

$$C_{Di} = \frac{C_L^2}{\pi A e} \quad (4)$$

Level Flight

Using these expressions for lift and drag, the case of level flight is analyzed. To maintain a constant altitude, the lift produced by the aircraft must equal the weight of the aircraft. For a given altitude and airspeed, this implies a required value of C_L . This value of C_L is given by

$$C_L = \frac{mg}{\frac{1}{2} \rho V^2 S} \quad (5)$$

So, the C_L required for level flight is a function of speed. From Eqs. (3) and (4), it is apparent that this implies a certain coefficient of drag. Substituting this coefficient of drag into Eq. (2) gives the drag for level flight as a function of speed:

$$D = C_{D0} \frac{1}{2} \rho V^2 S + \frac{(mg)^2}{\pi A e \frac{1}{2} \rho V^2 S} \quad (6)$$

Here, the first term represents the zero-lift drag (also called parasite drag) and the second term is the induced drag. These two terms are plotted along with the total drag in Fig. 1.

Turbulence

Atmospheric turbulence is typically modeled as filtered Gaussian white noise. The three components of turbulence (i.e., longitudinal, lateral and vertical) are modeled independently. The Dryden turbulence model is one commonly used atmospheric turbulence model [24]. It specifies the spectra of the three components of turbulence as follows:

$$\Phi_{u_g}(\Omega) = \sigma_u^2 \frac{2L_u}{\pi} \frac{1}{1 + (L_u \Omega)^2} \quad (7a)$$

$$\Phi_{v_g}(\Omega) = \sigma_v^2 \frac{L_v}{\pi} \frac{1 + 3(L_v \Omega)^2}{[1 + (L_v \Omega)^2]^2} \quad (7b)$$

$$\Phi_{w_g}(\Omega) = \sigma_w^2 \frac{L_w}{\pi} \frac{1 + 3(L_w \Omega)^2}{[1 + (L_w \Omega)^2]^2} \quad (7c)$$

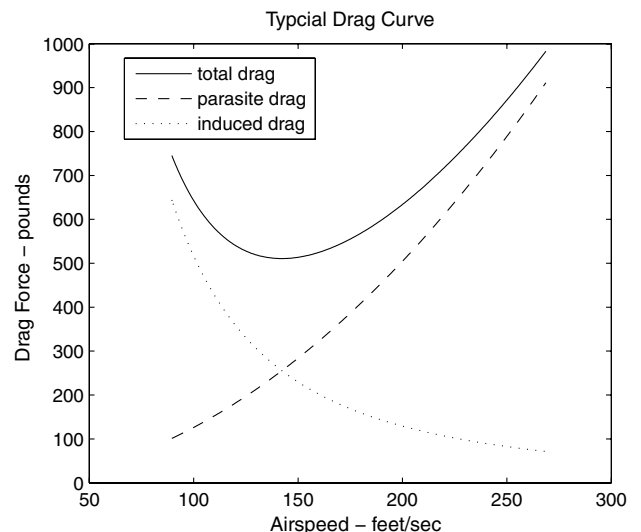


Fig. 1 Drag $D(V)$ in level flight.

The spectra are given in terms of spatial frequency, which is converted to temporal frequency ω by multiplying by the speed of the aircraft:

$$\omega = \Omega U_0 \quad (8)$$

At medium to high altitudes (above 2000 ft) the turbulence is assumed to be isotropic. The characteristic lengths and the intensities in each direction are equal to each other. A typical characteristic length is 1750 ft. Intensities are charted as a function of altitude. Moderate turbulence has a root-mean-square intensity of about 10 ft/s at 2000 ft, decreasing roughly linearly to near zero at 60,000 ft.

Whereas lateral turbulence has little effect on the speed of an aircraft, longitudinal turbulence has a direct effect on airspeed. Longitudinal turbulence with a spectrum matching that given in Eq. (7a) can be obtained by passing white noise through a filter of the form

$$\sigma_u \sqrt{\frac{2L_u}{U_0} \frac{1}{\frac{L_u}{U_0}s + 1}} \quad (9)$$

Vertical turbulence has an indirect effect on airspeed, but for this analysis it is ignored.

Control Design

Dynamic Model

Based on the aerodynamic model presented above, a simple dynamic model is considered: a scalar system perturbed by turbulence. The system is of the form

$$m \frac{dv}{dt} = -D(V) + bu \quad (10a)$$

$$\epsilon d\eta = -\eta dt + \sqrt{\epsilon} q dW \quad (10b)$$

The wind speed is defined as a headwind being positive, so that airspeed is the sum of groundspeed and wind speed. More precisely, airspeed is considered to be given by

$$V = v + asat\eta \quad (11)$$

where $asat\eta$ is the wind speed. The saturation function

$$\text{sat}(\eta) = \begin{cases} \eta & \text{if } -1 < \eta < 1 \\ 1 & \text{if } \eta \geq 1 \\ -1 & \text{if } \eta \leq -1 \end{cases} \quad (12)$$

is introduced for mathematical convenience. Its sole purpose is to ensure that the wind speed is bounded, which is a requirement for the stochastic averaging results used below. However, it is quite reasonable to bound the wind speed because it is not physically possible for the wind speed to be unbounded. The effect of the sat function can be made negligible by choosing q small with respect to one. The constant a can then be chosen to give the desired wind amplitude. The wind speed is modeled as filtered Gaussian white noise, as per the Dryden longitudinal turbulence model. The timescale of the turbulence ($\epsilon \triangleq L_u/U_0$) is taken to be a constant, using an airspeed representative of the range of airspeeds expected to be encountered.

Without loss of generality, the wind speed is taken as zero mean. If there were a steady-state component to the wind, then v would represent the ground speed plus the steady-state wind component, but the dynamics of the system would remain the same.

The rate of change of v is determined from total drag, engine thrust, and the mass of the aircraft. Engine thrust is modeled as proportional to the control input, namely throttle position. The drag function is taken as a general convex map with a minimum at speed v_* .

It is assumed that a proportional–integral control law is used to control airspeed to a setpoint \hat{v}_* . The control law is written as

$$u = k_p(\hat{v}_* - V) + k_i\sigma \quad (13a)$$

$$\frac{d\sigma}{dt} = \hat{v}_* - V \quad (13b)$$

Combining Eqs. (10) and (13), the aircraft model is written as follows:

$$m \frac{dv}{dt} = -D(V) + b[k_p(\hat{v}_* - V) + k_i\sigma] \quad (14a)$$

$$\frac{d\sigma}{dt} = \hat{v}_* - V \quad (14b)$$

$$\epsilon d\eta = -\eta dt + \sqrt{\epsilon} q dW \quad (14c)$$

In this model, $a, b, k_i, k_p, m, q, \hat{v}_*$, and ϵ are positive. The airspeed V can be measured by a pitot-static system. It is considered that dv/dt , the acceleration of the aircraft, can also be measured. Further, it is assumed that the thrust produced by the engine (i.e., bu) and the mass of the aircraft are known. In the control design below, this is used.

The aircraft model in Eq. (14) represents the quasi-steady dynamics of the aircraft with altitude tightly controlled. The underlying assumptions of this model are that altitude is being controlled with the elevator, and that the altitude response is much faster than the airspeed response. The assumptions are chosen to be consistent with a jet aircraft in slow flight. Using elevator to control the airspeed of a jet in slow flight can result in substantial loss of altitude, so altitude is maintained with elevator and throttle is used to control airspeed. The throttle response of a jet aircraft, especially at a low throttle setting, is slow. Because of this, the airspeed controller is assumed to have a much lower bandwidth than the altitude controller.

Turbulence-Based Extremum Seeking

The goal is to optimize endurance. It is assumed that fuel consumption is an increasing function of thrust and that the thrust vector is level with the flight path. Then, optimizing endurance is equivalent to minimizing throttle position. That is, the cost to be minimized is the control input u . Normally, this would require adding a perturbation to the setpoint of the system, \hat{v}_* . By modulating the cost with this perturbation signal, the rate of change of the cost with respect to \hat{v}_* would be estimated. The setpoint of the system would then be updated using an integral control law with a gain proportional to the estimated gradient. It is desired to do the same thing, but without adding a perturbation signal.

Observe that the goal of minimizing u is, more specifically, the goal of minimizing u in steady flight. Note that in steady flight Eq. (10a) reduces to $D(V) = bu$, so minimizing u in steady flight is equivalent to minimizing $D(V)$. Also, in steady flight Eq. (13b) reduces to $\hat{v}_* = V$. The goal can then be stated as choosing \hat{v}_* such that $D(\hat{v}_*)$ is minimized.

While drag is not directly measurable, from Eq. (10a) it is seen that drag is indirectly measurable. Using knowledge of vehicle acceleration, engine thrust, and mass, drag $D(V)$ is calculated as

$$D(V) = bu - m \frac{dv}{dt} \quad (15)$$

It is desired to demodulate this signal with the perturbation velocity. If the aircraft has a measurement of ground speed, say from an inertial navigation system, and a measurement of airspeed, the difference of the two could serve as a measurement of the perturbation. If the aircraft is not so equipped, it is possible to obtain an approximation of the airspeed perturbation from the error signal feeding the control law ($\hat{v}_* - V$). Here, the latter approach is taken. As in traditional extremum seeking, an integral control law is used to update the system and a gain proportional to this demodulated signal is chosen:

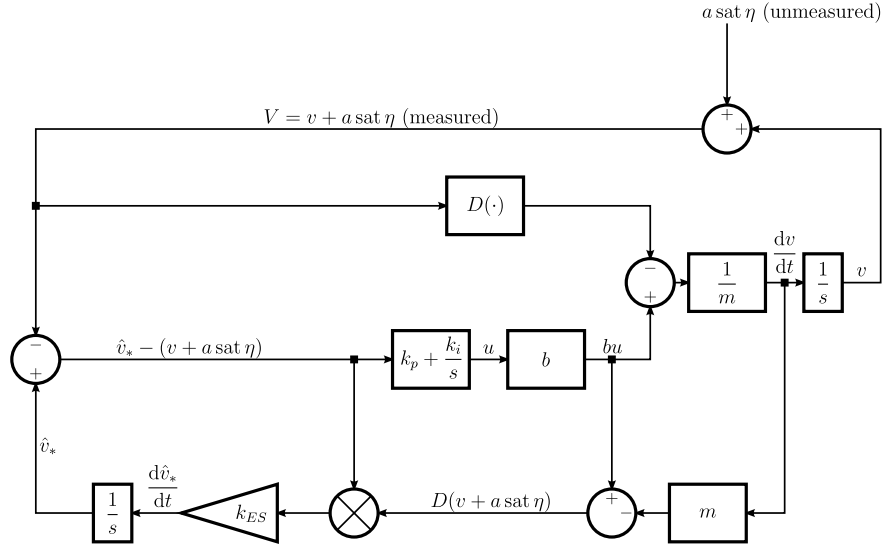


Fig. 2 Block diagram of system and extremum-seeking feedback. The algorithm uses measurements of dv/dt , bu , m , and $v + a \text{ sat } \eta$, but not of v and η alone.

$$\frac{d\hat{v}_*}{dt} = k_{ES}[\hat{v}_* - V] \left(bu - m \frac{dv}{dt} \right) \quad (16)$$

The system and extremum-seeking control law are shown in Fig. 2.

Analysis

In this section, analysis of the closed loop system formed by combining the aircraft model (14) with the extremum-seeking control law (16) is performed. For analysis, the expression $(bu - m dv/dt)$ in the control law is written simply as $D(V)$. The expression for V from Eq. (11) is also substituted throughout. This produces the following set of equations:

$$m \frac{dv}{dt} = -D(v + a \text{ sat } \eta) + b[k_p(\hat{v}_* - (v + a \text{ sat } \eta)) + k_i \sigma] \quad (17a)$$

$$\frac{d\sigma}{dt} = \hat{v}_* - (v + a \text{ sat } \eta) \quad (17b)$$

$$\frac{d\hat{v}_*}{dt} = k_{ES}[\hat{v}_* - (v + a \text{ sat } \eta)]D(v + a \text{ sat } \eta) \quad (17c)$$

$$\epsilon d\eta = -\eta dt + \sqrt{\epsilon} q dW \quad (17d)$$

Theorem 1: Consider system (17) composed of the aircraft model (10–13) and parameter update law (16), where $D(\cdot)$ is a convex map with a minimum at v_* , all constants are positive, and $K_{ES} \in (0, bk_p/m\bar{D}_*)$, where \bar{D}_* is a known upper bound on minimum drag, $D(v_*)$. Let constants C_2 and C_4 be defined by

$$C_2(q) \triangleq \frac{q^2}{2} \text{erf} \frac{1}{q} - \frac{q}{\sqrt{\pi}} e^{-\frac{1}{q^2}} + 1 - \text{erf} \frac{1}{q} \quad (18a)$$

$$C_4(q) \triangleq \frac{3}{4} q^4 \text{erf} \frac{1}{q} - \frac{q}{\sqrt{\pi}} e^{-\frac{1}{q^2}} \left(1 + \frac{3}{2} q^2 \right) + 1 - \text{erf} \frac{1}{q} \quad (18b)$$

Suppose $D(\cdot)$ is three times differentiable at v_* . Then there exists a constant a^* such that for any $0 < a < a^*$ there exist constants $r > 0$, $c > 0$, and $\gamma > 0$ and a function $T(\epsilon): (0, \epsilon_0) \rightarrow \mathbb{N}$ with the property $\lim_{\epsilon \rightarrow 0} T(\epsilon) = \infty$, such that for any initial condition $|\Delta^{\epsilon, a}(0)| < r$, and any $\delta > 0$,

$$\liminf_{\epsilon \rightarrow 0} \{t \geq 0: |\Delta^{\epsilon, a}(t)| > c|\Delta^{\epsilon, a}(0)|e^{-\gamma t} + O(a^3) + \delta\} = \infty, \text{ a.s.} \quad (19)$$

and

$$\lim_{\epsilon \rightarrow 0} P\{|\Delta^{\epsilon, a}(t)| \leq c|\Delta^{\epsilon, a}(0)|e^{-\gamma t} + O(a^3) + \delta \forall t \in [0, T(\epsilon)]\} = 1 \quad (20)$$

where

$$\Delta^{\epsilon, a}(t) \triangleq \begin{pmatrix} v(t) \\ \sigma(t) \\ \hat{v}_*(t) \end{pmatrix} - \begin{pmatrix} v_* - \frac{1}{6} \frac{D''(v_*)}{D'(v_*)} \frac{C_4}{C_2} a^2 \\ \frac{D(v_*)}{bk_i} + \frac{D'(v_*)}{2} \frac{C_2}{bk_i} a^2 \\ v_* - \frac{1}{6} \frac{D''(v_*)}{D'(v_*)} \frac{C_4}{C_2} a^2 \end{pmatrix}$$

Theorem 1 roughly states that choosing the gain K_{ES} as a small positive number causes the average airspeed to converge (both almost surely and in probability) to the minimum drag speed, with a small bias. The conditions for this are that the turbulence amplitude is small and the initial state of the aircraft is sufficiently close to the final average equilibrium. The remainder of this section is dedicated to the proof of Theorem 1. These equations are transformed into error variables that are expected to converge to near zero. Stochastic averaging is used on this error system to find the average system. Then the equilibrium of the average system is found and the stability of the equilibrium is tested. Throughout the analysis, drag is treated as a general convex map. No assumptions are made about the exact nature of the nonlinearity.

Error Variables

Define the error variables

$$v^e = v - v_* \quad (21a)$$

$$\sigma^e = \sigma - \frac{D(v_*)}{bk_i} \quad (21b)$$

$$\hat{v}_*^e = \hat{v}_* - v \quad (21c)$$

The fraction $D(v_*)/bk_i$ is the equilibrium value of the integrator when the aircraft is flying at the minimum drag speed with no disturbances. Also define

$$\chi(t) = \eta(\epsilon t) \quad (22a)$$

$$B(t) = \frac{1}{\sqrt{\epsilon}} W(\epsilon t) \tag{22b}$$

Then the error system is

$$m \frac{dv^e}{dt} = -D(v^e + v_* + \text{asat}\chi(t/\epsilon)) + b \left[k_p (\hat{v}_*^e - \text{asat}\chi(t/\epsilon)) + k_i \left(\sigma^e + \frac{D(v_*)}{bk_i} \right) \right] \tag{23a}$$

$$\frac{d\sigma^e}{dt} = \hat{v}_*^e - \text{asat}\chi(t/\epsilon) \tag{23b}$$

$$\begin{aligned} \frac{d\hat{v}_*^e}{dt} = \frac{d\hat{v}_*}{dt} - \frac{dv}{dt} &= k_{ES}[\hat{v}_*^e - \text{asat}\chi(t/\epsilon)]D(v^e + v_* + \text{asat}\chi(t/\epsilon)) \\ &- \frac{1}{m} \left\{ -D(v^e + v_* + \text{asat}\chi(t/\epsilon)) \right. \\ &\left. + b \left[k_p (\hat{v}_*^e - \text{asat}\chi(t/\epsilon)) + k_i \left(\sigma^e + \frac{D(v_*)}{bk_i} \right) \right] \right\} \end{aligned} \tag{23c}$$

$$d\chi(t) = -\chi(t)dt + qdB(t) \tag{23d}$$

Stochastic Averaging

Using stochastic averaging [5], the average system is then

$$m \frac{dv^{e,a}}{dt} = \int_{-\infty}^{\infty} -D(v^{e,a} + v_* + \text{asat}\eta)\mu(d\eta) + b \left[k_p \left(\hat{v}_*^{e,a} - \int_{-\infty}^{\infty} \text{asat}\eta\mu(d\eta) \right) + k_i \left(\sigma^{e,a} + \frac{D(v_*)}{bk_i} \right) \right] \tag{24a}$$

$$\frac{d\sigma^{e,a}}{dt} = \hat{v}_*^{e,a} - \int_{-\infty}^{\infty} \text{asat}\eta\mu(d\eta) \tag{24b}$$

$$\begin{aligned} \frac{d\hat{v}_*^{e,a}}{dt} &= \int_{-\infty}^{\infty} k_{ES}[\hat{v}_*^{e,a} - \text{asat}\eta] \times D(v^{e,a} + v_* + \text{asat}\eta)\mu(d\eta) \\ &- \frac{1}{m} \left\{ \int_{-\infty}^{\infty} -D(v^{e,a} + v_* + \text{asat}\eta)\mu(d\eta) \right. \\ &\left. + b \left[k_p \left(\hat{v}_*^{e,a} - \int_{-\infty}^{\infty} \text{asat}\eta\mu(d\eta) \right) + k_i \left(\sigma^{e,a} + \frac{D(v_*)}{bk_i} \right) \right] \right\} \end{aligned} \tag{24c}$$

where the invariant distribution of η is given by

$$\mu(d\eta) = \frac{1}{\sqrt{\pi q}} e^{-\frac{\eta^2}{q^2}} d\eta \tag{25}$$

To simplify these equations, a function $\bar{D}(\cdot)$ is introduced. This function is the same as $D(\cdot)$, but recentered around the minimum drag point:

$$\bar{D}(v^{e,a} + \text{asat}\eta) \equiv D(v^{e,a} + v_* + \text{asat}\eta) - D(v_*) \tag{26}$$

This new drag function is zero when its argument is zero:

$$\bar{D}(0) = 0 \tag{27}$$

The average system (24) is simplified using \bar{D} and noting that

$$\int_{-\infty}^{\infty} \text{asat}\eta\mu(d\eta) = 0 \tag{28}$$

This can be seen since sat is an odd function and μ is an even function, making the integrand odd; the integral from $-\infty$ to 0 cancels the integral from 0 to ∞ . The average system becomes the following:

$$m \frac{dv^{e,a}}{dt} = - \int_{-\infty}^{\infty} \bar{D}(v^{e,a} + \text{asat}\eta)\mu(d\eta) + b[k_p \hat{v}_*^{e,a} + k_i \sigma^{e,a}] \tag{29a}$$

$$\frac{d\sigma^{e,a}}{dt} = \hat{v}_*^{e,a} \tag{29b}$$

$$\begin{aligned} \frac{d\hat{v}_*^{e,a}}{dt} &= \int_{-\infty}^{\infty} k_{ES}[\hat{v}_*^{e,a} - \text{asat}\eta] \times [\bar{D}(v^{e,a} + \text{asat}\eta) + D(v_*)]\mu(d\eta) \\ &- \frac{1}{m} \left\{ - \int_{-\infty}^{\infty} \bar{D}(v^{e,a} + \text{asat}\eta)\mu(d\eta) + b[k_p \hat{v}_*^{e,a} + k_i \sigma^{e,a}] \right\} \end{aligned} \tag{29c}$$

Equilibrium of the Average System

To find the equilibrium of the average system, first observe from Eq. (29b) that the equilibrium value of $\hat{v}_*^{e,a}$ is zero, that is,

$$\hat{v}_{*eq}^{e,a} = 0 \tag{30}$$

Next, from Eq. (29c) it is seen that at equilibrium,

$$\begin{aligned} \int_{-\infty}^{\infty} k_{ES}[\hat{v}_{*eq}^{e,a} - \text{asat}\eta] \times [\bar{D}(v_{eq}^{e,a} + \text{asat}\eta) \\ + D(v_*)]\mu(d\eta) - \left(\frac{dv^{e,a}}{dt} \right)_{eq} = 0 \end{aligned} \tag{31}$$

Here, it has been noted that the second term in Eq. (29c) is just $(dv^{e,a}/dt)_{eq}$, which must be zero at equilibrium. After simplification, which employs Eqs. (28) and (30), the expression (31) reduces to

$$\int_{-\infty}^{\infty} \text{sat}\eta[\bar{D}(v_{eq}^{e,a} + \text{asat}\eta)]\mu(d\eta) = 0 \tag{32}$$

To solve this equation for $v_{eq}^{e,a}$, the process is similar to the proof of stability for a general nonlinear dynamic system presented in [5]. Two expansions are used: one for $v_{eq}^{e,a}$ in a and one for \bar{D} in $v_{eq}^{e,a}$. Take $v_{eq}^{e,a}$ in the form

$$v_{eq}^{e,a} = n_0 + n_1 a + n_2 a^2 + n_3 a^3 + O(a^4) \tag{33}$$

Also use an expansion of the drag function \bar{D} in terms of powers of its argument. Center the expansion around n_0 .

$$\begin{aligned} \bar{D}(v) &= \bar{D}(n_0) + \bar{D}'(n_0)(v - n_0) + \frac{\bar{D}''(n_0)}{2!}(v - n_0)^2 \\ &+ \frac{\bar{D}'''(n_0)}{3!}(v - n_0)^3 + O((v - n_0)^4) \end{aligned} \tag{34}$$

Using these expansions for $v_{eq}^{e,a}$ and \bar{D} , the condition for equilibrium in Eq. (32) becomes

$$\begin{aligned} \int_{-\infty}^{\infty} \text{sat}\eta[\bar{D}(v_{eq}^{e,a} + \text{asat}\eta)]\mu(d\eta) &= \int_{-\infty}^{\infty} \text{sat}\eta \left[\bar{D}(n_0) \right. \\ &+ \bar{D}'(n_0)(n_1 a + n_2 a^2 + n_3 a^3 + O(a^4) + \text{asat}\eta) \\ &+ \frac{\bar{D}''(n_0)}{2!}(n_1 a + n_2 a^2 + n_3 a^3 + O(a^4) + \text{asat}\eta)^2 \\ &+ \frac{\bar{D}'''(n_0)}{3!}(n_1 a + n_2 a^2 + n_3 a^3 + O(a^4) + \text{asat}\eta)^3 \\ &\left. + O((n_1 a + n_2 a^2 + n_3 a^3 + O(a^4) + \text{asat}\eta)^4) \right] \mu(d\eta) \\ &= \bar{D}'(n_0)((C_2)a) + \frac{\bar{D}''(n_0)}{2!}((2n_2 C_2)a^3 + (2n_1 C_2)a^2) \\ &+ \frac{\bar{D}'''(n_0)}{3!}(3n_1^2 C_2 + C_4)a^3 + O(a^4) = 0 \end{aligned} \tag{35}$$

Here, the following integrals have been used:

$$\int_{-\infty}^{\infty} \text{sat}^{2k+1} \eta \mu(d\eta) = 0, \quad \text{where } k = 0, 1, 2, \dots \quad (36a)$$

$$\int_{-\infty}^{\infty} \text{sat}^2 \eta \mu(d\eta) = \frac{q^2}{2} \operatorname{erf} \frac{1}{q} - \frac{q}{\sqrt{\pi}} e^{-\frac{1}{q^2}} + 1 - \operatorname{erf} \frac{1}{q} \triangleq C_2(q) \quad (36b)$$

$$\int_{-\infty}^{\infty} \text{sat}^4 \eta \mu(d\eta) = \frac{3}{4} q^4 \operatorname{erf} \frac{1}{q} - \frac{q}{\sqrt{\pi}} e^{-\frac{1}{q^2}} \left(1 + \frac{3}{2} q^2\right) + 1 - \operatorname{erf} \frac{1}{q} \triangleq C_4(q) \quad (36c)$$

To help understand the expressions for C_2 and C_4 , note that C_2 and C_4 can be approximated by

$$C_2(q) \approx \frac{q^2}{2} \quad (37a)$$

$$C_4(q) \approx \frac{3}{4} q^4 \quad (37b)$$

for small q . For q smaller than 0.5, the approximation for C_2 is accurate to within 1% and the approximation for C_4 is accurate to within 3%. Both C_2 and C_4 are zero when q is zero, and monotonically approach 1 as q grows without bound.

Because the expression in Eq. (35) is a polynomial in a , and the polynomial is equal to zero, each of the coefficients of a must be zero. This gives the following system of equations:

$$a^1: \bar{D}'(n_0)C_2 = 0 \quad (38a)$$

$$a^2: \bar{D}''(n_0)n_1C_2 = 0 \quad (38b)$$

$$a^3: \bar{D}''(n_0)n_2C_2 + \frac{\bar{D}'''(n_0)}{3!}(3n_1^2C_2 + C_4) = 0 \quad (38c)$$

Since \bar{D} is assumed convex, its first derivative can only be zero when evaluated at a minimum point. Noting this, and that \bar{D} has been defined with its minimum at zero, the solution to this set of equations is

$$n_0 = 0 \quad (39a)$$

$$n_1 = 0 \quad (39b)$$

$$n_2 = -\frac{1}{6} \frac{\bar{D}'''(0)C_4}{\bar{D}''(0)C_2} \quad (39c)$$

so an $\mathcal{O}(a^3)$ expression for $v_{\text{eq}}^{e,a}$ is

$$v_{\text{eq}}^{e,a} = -\frac{1}{6} \frac{\bar{D}'''(0)C_4(q)}{\bar{D}''(0)C_2(q)} a^2 + \mathcal{O}(a^3) \quad (40)$$

Recalling Eq. (37), it is noted that for small q the following is obtained:

$$v_{\text{eq}}^{e,a} = -\frac{1}{4} \frac{\bar{D}'''(0)}{\bar{D}''(0)} q^2 a^2$$

Next, using the expression (40) for $v_{\text{eq}}^{e,a}$, Eq. (29a) is set equal to zero and solved for $\sigma_{\text{eq}}^{e,a}$. This time a lower-order expansion for \bar{D} is used:

$$\bar{D}(v) = \bar{D}(0) + \bar{D}'(0)v + \frac{\bar{D}''(0)}{2!} v^2 + \mathcal{O}(v^3) \quad (41)$$

The function \bar{D} has been defined so that it has a minimum at the origin, so the first two terms of the expansion are zero and the expression is simplified to

$$\bar{D}(v) = \frac{\bar{D}''(0)}{2!} v^2 + \mathcal{O}(v^3) \quad (42)$$

Using these expressions for $v_{\text{eq}}^{e,a}$ and \bar{D} , the condition for equilibrium in Eq. (29a) becomes

$$\begin{aligned} & \int_{-\infty}^{\infty} -\bar{D}(v_{\text{eq}}^{e,a} + \text{asat}\eta)\mu(d\eta) + b[k_p \hat{v}_{* \text{eq}}^{e,a} + k_i \sigma_{\text{eq}}^{e,a}] \\ &= \int_{-\infty}^{\infty} -\frac{\bar{D}''(0)}{2!} (n_2 a^2 + \mathcal{O}(a^3) + \text{asat}\eta)^2 \\ & \quad + \mathcal{O}((n_2 a^2 + \mathcal{O}(a^3) + \text{asat}\eta)^3)\mu(d\eta) + b k_i \sigma_{\text{eq}}^{e,a} \\ &= -\frac{\bar{D}''(0)}{2!} (C_2) a^2 + \mathcal{O}(a^3) + b k_i \sigma_{\text{eq}}^{e,a} = 0 \end{aligned} \quad (43)$$

which gives

$$\sigma_{\text{eq}}^{e,a} = \frac{\bar{D}''(0)C_2}{2bk_i} a^2 + \mathcal{O}(a^3) \quad (44)$$

So an equilibrium of the average system in terms of the error variables has been found. Collecting the expressions in Eqs. (30), (40), and (44), the equilibrium is expressed as the following:

$$v_{\text{eq}}^{e,a} = -\frac{1}{6} \frac{\bar{D}'''(0)C_4}{\bar{D}''(0)C_2} a^2 + \mathcal{O}(a^3) \quad (45a)$$

$$\sigma_{\text{eq}}^{e,a} = \frac{\bar{D}''(0)C_2}{2bk_i} a^2 + \mathcal{O}(a^3) \quad (45b)$$

$$\hat{v}_{* \text{eq}}^{e,a} = 0 \quad (45c)$$

Converting back to the original variables, the equilibrium of the average system is the following:

$$v_{\text{eq}}^a = v_* - \frac{1}{6} \frac{D'''(v_*)C_4}{D''(v_*)C_2} a^2 + \mathcal{O}(a^3) \quad (46a)$$

$$\sigma_{\text{eq}}^a = \frac{D(v_*)}{bk_i} + \frac{D''(v_*)C_2}{2bk_i} a^2 + \mathcal{O}(a^3) \quad (46b)$$

$$\hat{v}_{* \text{eq}}^a = v_{\text{eq}}^a \quad (46c)$$

For small disturbance magnitudes (i.e., small a) the average speed of the system has an equilibrium point at the minimum drag speed, v_* . The deviation from the minimum drag speed is proportional to the third derivative of the drag curve at the minimum drag speed and decreases with a^2 . If the drag curve is asymmetric, the speed bias is to the flatter side of the drag curve relative to the minimum drag point.

Stability of the Equilibrium

To determine the stability of the equilibrium, the average system (29) is linearized around the equilibrium point and the linearized system is tested for stability.

The Jacobian of the average system (29) at the equilibrium point in terms of the error variables ($v^{e,a}$, $\sigma^{e,a}$, $\hat{v}_*^{e,a}$) is

$$J = \begin{pmatrix} J_{1,1} & \frac{bk_i}{m} & \frac{bk_p}{m} \\ 0 & 0 & 1 \\ J_{3,1} & -\frac{bk_i}{m} & J_{3,3} \end{pmatrix} \quad (47a)$$

where $J_{1,1}$, $J_{3,1}$, and $J_{3,3}$ are given by

$$J_{1,1} = \frac{1}{m} \int_{-\infty}^{\infty} -\bar{D}'(v_{\text{eq}}^{e,a} + \text{asat}\eta)\mu(d\eta) \tag{47b}$$

$$J_{3,1} = \int_{-\infty}^{\infty} k_{\text{ES}}[\hat{v}_{* \text{eq}}^{e,a} - \text{asat}\eta] \times [\bar{D}'(v_{\text{eq}}^{e,a} + \text{asat}\eta)]\mu(d\eta) - \frac{1}{m} \int_{-\infty}^{\infty} -\bar{D}'(v_{\text{eq}}^{e,a} + \text{asat}\eta)\mu(d\eta) \tag{47c}$$

$$J_{3,3} = \int_{-\infty}^{\infty} k_{\text{ES}}[\bar{D}(v_{\text{eq}}^{e,a} + \text{asat}\eta) + D(v_*)]\mu(d\eta) - \frac{bk_p}{m} \tag{47d}$$

The characteristic equation of the system is given by $\det(sI - J) = 0$, or

$$\begin{vmatrix} s - J_{1,1} & -\frac{bk_i}{m} & -\frac{bk_p}{m} \\ 0 & s & -1 \\ -J_{3,1} & \frac{bk_i}{m} & s - J_{3,3} \end{vmatrix} = 0 \tag{48}$$

Writing this as a polynomial, the characteristic equation is as follows.

$$s^3 - (J_{1,1} + J_{3,3})s^2 + \left(J_{1,1}J_{3,3} - \frac{bk_p}{m}J_{3,1} + \frac{bk_i}{m} \right)s - \frac{bk_i}{m}(J_{1,1} + J_{3,1}) = 0 \tag{49}$$

By applying Routh's criterion, it is seen that the system is stable if each of the coefficients in the characteristic polynomial are positive and the product of the s^2 and s^1 coefficients is greater than the product of the s^3 and s^0 coefficients. To test this expressions for $J_{1,1}$, $J_{3,1}$, and $J_{3,3}$ are required. Expressions accurate to $O(a^3)$ are found for each.

First, $J_{1,1}$ is found. Using the expressions $v_{\text{eq}}^{e,a} = n_2a^2 + O(a^3)$ and $\bar{D}'(v) = \bar{D}''(0)v + \frac{\bar{D}'''(0)}{2!}v^2 + O(v^3)$ the following is obtained:

$$\begin{aligned} J_{1,1} &= \frac{1}{m} \int_{-\infty}^{\infty} -\bar{D}'(v_{\text{eq}}^{e,a} + \text{asat}\eta)\mu(d\eta) \\ &= -\frac{1}{m} \int_{-\infty}^{\infty} \bar{D}''(0)(n_2a^2 + O(a^3) + \text{asat}\eta) \\ &\quad + \frac{\bar{D}'''(0)}{2!}(n_2a^2 + O(a^3) + \text{asat}\eta)^2 \\ &\quad + O((n_2a^2 + O(a^3) + \text{asat}\eta)^3)\mu(d\eta) \\ &= -\frac{1}{m} \left[\bar{D}''(0)n_2 + \frac{\bar{D}'''(0)}{2!}C_2 \right] a^2 + O(a^3) \end{aligned} \tag{50}$$

Next, using the same expression for $v_{\text{eq}}^{e,a}$ and $\bar{D}'(v) = \bar{D}''(0)v + O(v^2)$ the expression for $J_{3,1}$ is found. Note that the second term in the original expression for $J_{3,1}$ is the negative of $J_{1,1}$:

$$\begin{aligned} J_{3,1} &= \int_{-\infty}^{\infty} k_{\text{ES}}[\hat{v}_{* \text{eq}}^{e,a} - \text{asat}\eta] \times [\bar{D}'(v_{\text{eq}}^{e,a} + \text{asat}\eta)]\mu(d\eta) \\ &\quad - \frac{1}{m} \int_{-\infty}^{\infty} -\bar{D}'(v_{\text{eq}}^{e,a} + \text{asat}\eta)\mu(d\eta) \\ &= -\int_{-\infty}^{\infty} k_{\text{ES}}\text{asat}\eta \times [\bar{D}''(0)(n_2a^2 + O(a^3) + \text{asat}\eta) \\ &\quad + O((n_2a^2 + O(a^3) + \text{asat}\eta)^2)]\mu(d\eta) - J_{1,1} \\ &= \left[-k_{\text{ES}}\bar{D}''(0)C_2 + \frac{1}{m} \left(\bar{D}''(0)n_2 + \frac{\bar{D}'''(0)}{2!}C_2 \right) \right] a^2 + O(a^3) \end{aligned} \tag{51}$$

Finally, an expression for $J_{3,3}$ is found. Here, the approximations $v_{\text{eq}}^{e,a} = 0 + O(a^2)$ and $\bar{D}(v) = \frac{\bar{D}''(0)}{2!}v^2 + O(v^3)$ are used. Then $J_{3,3}$ can be expressed as

$$\begin{aligned} J_{3,3} &= \int_{-\infty}^{\infty} k_{\text{ES}}[\bar{D}(v_{\text{eq}}^{e,a} + \text{asat}\eta) + D(v_*)]\mu(d\eta) - \frac{bk_p}{m} \\ &= \int_{-\infty}^{\infty} k_{\text{ES}} \left[\frac{\bar{D}''(0)}{2!}(O(a^2) + \text{asat}\eta)^2 + O((O(a^2) + \text{asat}\eta)^3) \right. \\ &\quad \left. + D(v_*) \right] \mu(d\eta) - \frac{bk_p}{m} = \left[k_{\text{ES}}D(v_*) - \frac{bk_p}{m} \right] \\ &\quad + \left[k_{\text{ES}} \frac{\bar{D}''(0)}{2!}C_2 \right] a^2 + O(a^3) \end{aligned} \tag{52}$$

Now, using these expressions for the components of the Jacobian of the system, it is possible to calculate the coefficients in the characteristic equation and test for stability:

$$\begin{aligned} s^2: & -(J_{1,1} + J_{3,3}) \\ &= -\left(-\frac{1}{m} \left[\bar{D}''(0)n_2 + \frac{\bar{D}'''(0)}{2!}C_2 \right] a^2 + O(a^3) \right) \\ &\quad - \left(\left[k_{\text{ES}}D(v_*) - \frac{bk_p}{m} \right] + \left[k_{\text{ES}} \frac{\bar{D}''(0)}{2!}C_2 \right] a^2 + O(a^3) \right) \\ &= \left[\frac{bk_p}{m} - k_{\text{ES}}D(v_*) \right] + \left[\frac{1}{m} \left(\bar{D}''(0)n_2 + \frac{\bar{D}'''(0)}{2!}C_2 \right) \right. \\ &\quad \left. - k_{\text{ES}} \frac{\bar{D}''(0)}{2!}C_2 \right] a^2 + O(a^3) \end{aligned} \tag{53}$$

$$\begin{aligned} s^1: & J_{1,1}J_{3,3} - \frac{bk_p}{m}J_{3,1} + \frac{bk_i}{m} \\ &= \left(-\frac{1}{m} \left[\bar{D}''(0)n_2 + \frac{\bar{D}'''(0)}{2!}C_2 \right] a^2 + O(a^3) \right) \\ &\quad \times \left(\left[k_{\text{ES}}D(v_*) - \frac{bk_p}{m} \right] + \left[k_{\text{ES}} \frac{\bar{D}''(0)}{2!}C_2 \right] a^2 + O(a^3) \right) \\ &\quad - \frac{bk_p}{m} \left\{ \left[-k_{\text{ES}}\bar{D}''(0)C_2 + \frac{1}{m} \left(\bar{D}''(0)n_2 + \frac{\bar{D}'''(0)}{2!}C_2 \right) \right] a^2 \right. \\ &\quad \left. + O(a^3) \right\} + \frac{bk_i}{m} = \frac{bk_i}{m} + \left[-\frac{1}{m}k_{\text{ES}}D(v_*) \left(\bar{D}''(0)n_2 + \frac{\bar{D}'''(0)}{2!}C_2 \right) \right. \\ &\quad \left. - \frac{bk_p}{m}[-k_{\text{ES}}\bar{D}''(0)C_2] \right] a^2 + O(a^3) \end{aligned} \tag{54}$$

$$\begin{aligned} s^0: & -\frac{bk_i}{m}(J_{1,1} + J_{3,1}) \\ &= -\frac{bk_i}{m} \left(-\frac{1}{m} \left[\bar{D}''(0)n_2 + \frac{\bar{D}'''(0)}{2!}C_2 \right] a^2 + O(a^3) \right) \\ &\quad - \frac{bk_i}{m} \left\{ \left[-k_{\text{ES}}\bar{D}''(0)C_2 + \frac{1}{m} \left(\bar{D}''(0)n_2 + \frac{\bar{D}'''(0)}{2!}C_2 \right) \right] a^2 \right. \\ &\quad \left. + O(a^3) \right\} = \frac{bk_i}{m} [k_{\text{ES}}\bar{D}''(0)C_2] a^2 + O(a^3) \end{aligned} \tag{55}$$

So the characteristic equation of the average system can be written as

$$\begin{aligned} s^3 &+ \left\{ \left[\frac{bk_p}{m} - k_{\text{ES}}D(v_*) \right] \right. \\ &\quad \left. + \left[\frac{1}{m} \left(\bar{D}''(0)n_2 + \frac{\bar{D}'''(0)}{2!}C_2 \right) - k_{\text{ES}} \frac{\bar{D}''(0)}{2!}C_2 \right] a^2 + O(a^3) \right\} s^2 \\ &+ \left\{ \frac{bk_i}{m} + \left[-\frac{1}{m}k_{\text{ES}}D(v_*) \left(\bar{D}''(0)n_2 + \frac{\bar{D}'''(0)}{2!}C_2 \right) \right. \right. \\ &\quad \left. \left. - \frac{bk_p}{m}[-k_{\text{ES}}\bar{D}''(0)C_2] \right] a^2 + O(a^3) \right\} s \\ &+ \left\{ \frac{bk_i}{m} [k_{\text{ES}}\bar{D}''(0)C_2] a^2 + O(a^3) \right\} = 0 \end{aligned} \tag{56}$$

or, more simply, as

$$s^3 + \left\{ \left[\frac{bk_p}{m} - k_{ES}D(v_*) \right] + O(a^2) \right\} s^2 + \left\{ \frac{bk_i}{m} + O(a^2) \right\} s + \left\{ \frac{bk_i}{m} [k_{ES}\bar{D}''(0)C_2]a^2 + O(a^3) \right\} = 0 \quad (57)$$

The first step in checking for stability is to ensure that all of the coefficients of this polynomial are positive. Since all of the constants in this polynomial are assumed positive, for small a the coefficients are all positive if

$$0 < k_{ES} < \frac{bk_p}{mD(v_*)} \quad (58)$$

It must also be ensured that the product of the s^2 and s^1 coefficients is greater than the product of the s^3 and s^0 coefficients:

$$\left\{ \left[\frac{bk_p}{m} - k_{ES}D(v_*) \right] + O(a^2) \right\} \left\{ \frac{bk_i}{m} + O(a^2) \right\} > \left\{ \frac{bk_i}{m} [k_{ES}\bar{D}''(0)C_2]a^2 + O(a^3) \right\} \quad (59)$$

By making an $O(a^2)$ approximation, this reduces to

$$\frac{bk_i}{m} \left(\frac{bk_p}{m} - k_{ES}D(v_*) \right) > O(a^2) \quad (60)$$

which is true for small a if Eq. (58) is satisfied. So, by Routh's criterion, the linearized average system is stable for small a if k_{ES} is chosen small enough to satisfy Eq. (58).

The stability of the linearized average system implies stability of the nonlinear perturbed system. Because the linearized average system is stable, the nonlinear average system (29) is locally exponentially stable (Corollary 4.3 in [25]). From the stochastic averaging results in [5], exponential stability of the average system implies that the system is weakly exponentially stable under the random perturbation. This result is formalized in Theorem 1. The stability analysis concludes that turbulence-based extremum seeking stabilizes the aircraft to the the speed for optimal endurance.

Simulations

A simulation run using Simulink is presented here. The simulation follows Eq. (17) closely, with the addition of a high-pass filter and a low-pass filter. Although not necessary for stability, the use of a high-pass filter has been shown to improve the rate of convergence in other extremum-seeking applications [5]. Here, the high-pass filter is applied to the drag signal in the extremum-seeking loop. A low-pass filter is also added to smooth the controller. The filters are shown in Fig. 3. The parameters used in simulation are listed in Table 1. A plot of the simulation results is shown in Fig. 4.

For a direct comparison with the above analysis, a simulation without the high-pass and low-pass filters is presented in Fig. 5. The simulation parameters are the same as in Table 1, except that the filter time constants are not applicable and k_{ES} must be chosen much smaller. The stability limit for k_{ES} can be calculated using Theorem 1 and the simulation parameters in Table 1. For the simulation k_{ES} was chosen to be one-eighth of its stability limit. Numerical values for the stability limit of k_{ES} and k_{ES} itself are shown in Table 2. Also shown in Table 2 are the predicted equilibrium point and Jacobian matrix of the average system, corresponding to Eqs. (46) and (47), respectively. The Jacobian elements $J_{1,1}$, $J_{3,1}$ and $J_{3,3}$ are calculated using the $O(a^3)$ approximations given in Eqs. (50–52).

Discussion

The turbulence-based extremum-seeking algorithm successfully stabilizes the aircraft model to the airspeed for optimal endurance, with an average bias proportional to the third derivative of the drag curve and the square of turbulence intensity. The extremum-seeking controller does this without adding a perturbation to the setpoint of the system. Simulations conducted using a quadratic drag polar show little bias from the true minimum. The drag curve used in simulation is the same shown in Fig. 1. Note that while a quadratic drag polar is used, the drag curve is a nonpolynomial function of airspeed and contains higher order terms sufficient to investigate the bias of the estimated minimum drag speed predicted by Theorem 1.

The simulation demonstrates performance in turbulence with a root-mean-square amplitude of 3 ft/ sec, which represents light to moderate turbulence at most altitudes. This raises the question of how the controller will perform in other turbulence intensities. As shown in analysis, the steady-state bias improves as the turbulence intensity decreases. This is limited only by the fidelity of the accelerometer reading and the accuracy of the thrust and weight estimates. However, for any given k_{ES} the rate of convergence to the minimum drag speed also decreases with the turbulence intensity. Because encounters with turbulence are typically fairly short, on the order of minutes, it is desirable to increase the rate of convergence as

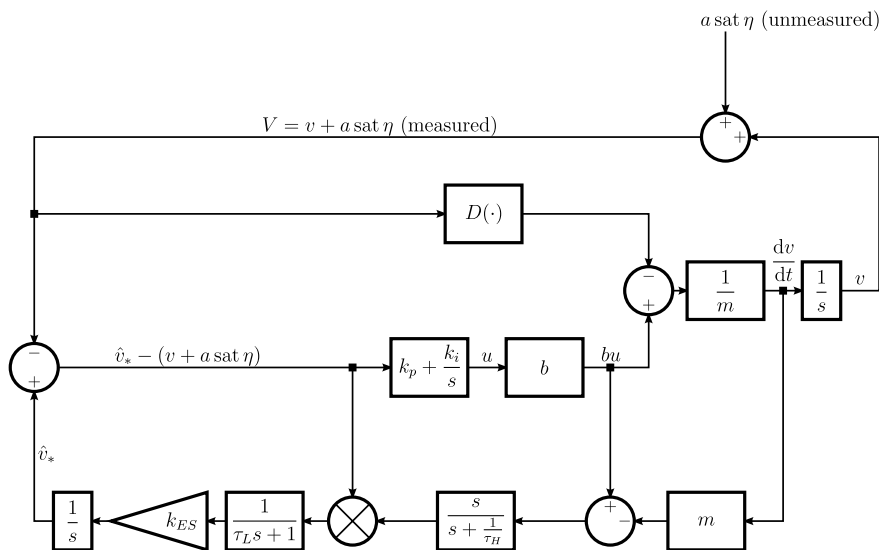


Fig. 3 Block diagram of the control system as simulated, including added filters.

Table 1 Simulation parameters

Parameter	Value	Units
σ_u	3	ft/s
L_u	1750	ft
U_0	142	ft/s
a	149	ft/s
q	0.0285	$s^{-1/2}$
ϵ	12.30	s
mg	14,300	lb
m	444	slugs
b	100	lbf/deg
k_p	2.22	deg/(ft/s)
k_i	0.0111	deg/[(ft/s) · s]
k_{ES}	1	[(ft/s)/s]/[(ft/s) · lbf]
τ_H	2	s
τ_L	5	s
$D(V)$	$(5.17 \times 10^6)V^2 + (0.0126)/V^2$	lbf (as in Fig. 1)
v_*	142.2	ft/s

Table 2 Parameters for simulation without filters

Parameter	Value	Units
$bk_p/mD(v_*)$	9.790×10^{-4}	[(ft/s)/s]/[(ft/s) · lbf]
k_{ES}	1.224×10^{-4}	[(ft/s)/s]/[(ft/s) · lbf]
v_{eq}^a	142.3	ft/s
σ_{eq}^a	460.4	(ft/s) · s
\hat{v}_{*eq}^a	142.3	ft/s
$J_{1,1}$	-2.640×10^{-21}	s^{-1}
$J_{1,2}$	0.0025	s^{-2}
$J_{1,3}$	0.5	s^{-1}
$J_{2,1}$	0	None
$J_{2,2}$	0	s^{-1}
$J_{2,3}$	1	None
$J_{3,1}$	-1.112×10^{-4}	s^{-1}
$J_{3,2}$	-0.0025	s^{-2}
$J_{3,3}$	-0.4374	s^{-1}

much as possible. This can be accomplished by increasing k_{ES} . Care should be taken, though, not to increase k_{ES} too much. The analytical stability result from Theorem 1 is stated in terms of the limiting case as a tends to zero. It is expected that the upper stability bound on k_{ES} will decrease as a increases, implying that k_{ES} should be chosen conservatively to prevent the system from becoming unstable in severe turbulence.

The issue of rate of convergence also demonstrates the necessity of using the high-pass and low-pass filters. The filters improve the rate of convergence by orders of magnitude. Indeed without them, the control design is not practical. The analysis above considers the simpler control design for improved clarity in the analysis. Omitting the filters keeps the basic style of analysis and functionality of the controller from being lost in the details.

A limitation of this work is that vertical gusts have been ignored. The results in [26], which show the potential robustness of extremum-seeking control to stochastic disturbances, suggest that vertical gusts may be handled well by this control scheme. Including vertical gusts in future analysis and simulations would increase confidence that the turbulence-based extremum-seeking controller will function as desired in real turbulence. A related limitation is that longitudinal aircraft dynamics are not modeled in simulation. This prevents the simulation from testing the validity of neglecting altitude dynamics.

The advantage of a turbulence-based approach, that it operates without using a perturbation signal, is also its disadvantage. Particularly at higher altitudes, an aircraft may not experience turbulence

often. Furthermore, the optimal airspeed varies with the weight of the aircraft, and possibly also with other flight parameters. Because of this, the current optimal airspeed may not be the same as the optimal airspeed found during the last encounter with turbulence. To address these issues, an application of turbulence-based extremum seeking would need to provide means of recording optimal speeds found during encounters with turbulence and extrapolating the recorded speeds to the current flight condition.

Another facet of this application that may prove complicated involves the varying curvature of the drag profile with altitude and weight. To achieve rapid convergence to the optimal speed across the flight envelope would require scheduling the extremum-seeking gain. Alternately, an extremum-seeking control law could be developed that was insensitive to the curvature of the drag profile. Such a method is developed in [27] for traditional sinusoidal-perturbation-based extremum seeking. Adapting this method for stochastic extremum-seeking schemes is a subject of current research.

Finally, it is noted that while the assumptions made in this paper apply to a jet aircraft, it may be possible to modify the controller for propeller aircraft. For jet aircraft, flight at the best lift-to-drag ratio results in maximum endurance, but for propeller aircraft maximum endurance is obtained at the minimum power speed. An extremum-seeking controller for propeller aircraft may be created by substituting an estimate of required power for the estimated drag. This can be accomplished by multiplying the drag estimate in the extremum-seeking controller by the measured airspeed.

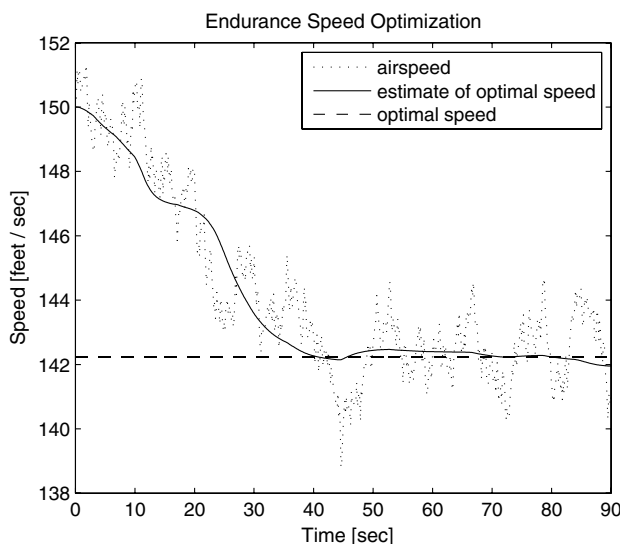


Fig. 4 Simulation results of endurance speed optimization.

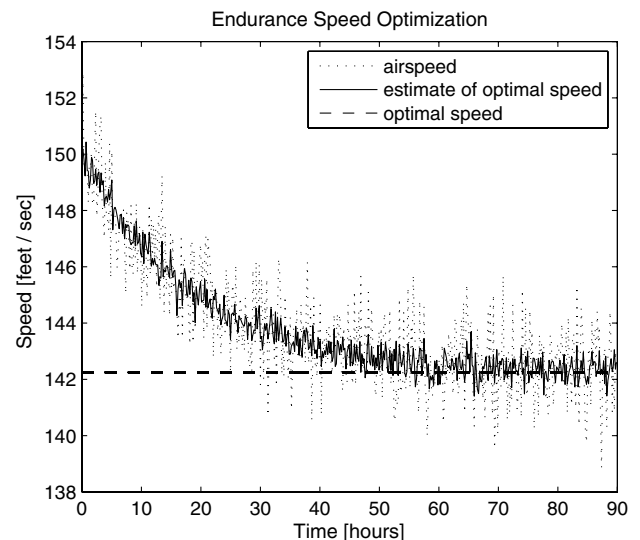


Fig. 5 Simulation results without added filters. By comparison with Fig. 4 it is clear that convergence can be sped up by several orders of magnitude by the addition of the filters.

Conclusions

A turbulence-based form of extremum seeking has been developed for optimizing the speed of an aircraft for maximum endurance. The turbulence-based approach allows extremum seeking to be performed without introducing an external perturbation. Assuming longitudinal turbulence in level flight and a general convex drag curve, analysis shows weak exponential stability to the minimum drag speed. Simulations show similar behavior with high-pass and low-pass filters added to the extremum-seeking loop.

References

- [1] Ariyur, K. B., and Krstic, M., "SISO Scheme and Linear Analysis," *Real-Time Optimization by Extremum-Seeking Control*, Wiley, Hoboken, NJ, 2003.
- [2] Wang, H.-H., and Krstic, M., "Extremum Seeking for Limit Cycle Minimization," *IEEE Transactions on Automatic Control*, Vol. 45, No. 12, Dec. 2000, pp. 2432–2436. doi:10.1109/9.895589
- [3] Choi, J.-Y., Krstic, M., Ariyur, K. B., and Lee, J. S., "Extremum Seeking Control for Discrete-Time Systems," *IEEE Transactions on Automatic Control*, Vol. 47, No. 2, Feb. 2002, pp. 318–323. doi:10.1109/9.983370
- [4] Tan, Y., Netic, D., and Mareels, I., "On the Choice of Dither in Extremum Seeking Systems: A Case Study," *Automatica*, Vol. 44, No. 5, 2008, pp. 1446–1450. doi:10.1016/j.automatica.2007.10.016
- [5] Liu, S.-J., and Krstic, M., "Stochastic Averaging in Continuous Time and Its Applications to Extremum Seeking," *IEEE Transactions on Automatic Control*, Vol. 55, No. 10, Oct. 2010, pp. 2235–2250. doi:10.1109/TAC.2010.2043290
- [6] Manzie, C., and Krstic, M., "Extremum Seeking With Stochastic Perturbations," *IEEE Transactions on Automatic Control*, Vol. 54, No. 3, March 2009, pp. 580–585. doi:10.1109/TAC.2008.2008320
- [7] Carnevale, D., Astolfi, A., Centioli, C., Podda, S., Vitale, V., and Zaccarian, L., "A New Extremum Seeking Technique and Its Application To Maximize RF Heating on FTU," *Fusion Engineering and Design*, Vol. 84, No. 2–6, 2009, pp. 554–558. doi:10.1016/j.fusengdes.2008.12.032
- [8] Tanelli, M., Astolfi, A., and Savaresi, S. M., "Non-Local Extremum Seeking Control for Active Braking Control Systems," *Proceedings of the 2006 IEEE International Conference on Control Applications*, IEEE Publ., Piscataway, NJ, 2006, pp. 891–896. doi:10.1109/CACSD-CCA-ISIC.2006.4776763
- [9] Schuster, E., Xu, C., Torres, N., Morinaga, E., Allen, C., and Krstic, M., "Beam Matching Adaptive Control via Extremum Seeking," *Nuclear Instruments and Methods in Physics Research. Section A: Accelerators, Spectrometers, Detectors and Associated Equipment*, Vol. 581, No. 3, 2007, pp. 799–815. doi:10.1016/j.nima.2007.07.154
- [10] Wang, H.-H., Yeung, S., and Krstic, M., "Experimental Application of Extremum Seeking on an Axial-Flow Compressor," *IEEE Transactions on Control Systems Technology*, Vol. 8, No. 2, March 2000, pp. 300–309. doi:10.1109/87.826801
- [11] Banaszuk, A., Ariyur, K. B., Krstic, M., and Jacobson, C. A., "An Adaptive Algorithm for Control of Combustion Instability," *Automatica*, Vol. 40, No. 11, 2004, pp. 1965–1972. doi:10.1016/j.automatica.2004.06.008
- [12] Moeck, J. P., Bothien, M. R., Paschereit, C. O., Gelbert, G., and King, R., "Two-Parameter Extremum Seeking for Control of Thermoacoustic Instabilities and Characterization of Linear Growth," *AIAA Paper 2007-1416*, Jan. 2007.
- [13] Becker, R., King, R., Petz, R., and Nitsche, W., "Adaptive Closed-Loop Separation Control on a High-Lift Configuration Using Extremum Seeking," *AIAA Journal*, Vol. 45, No. 6, 2007, pp. 1382–1392. doi:10.2514/1.24941
- [14] Bastin, G., Nešić, D., Tan, Y., and Mareels, I., "On Extremum Seeking in Bioprocesses with Multivalued Cost Functions," *Biotechnology Progress*, Vol. 25, No. 3, 2009, pp. 683–689. doi:10.1002/btpr.87
- [15] Ou, Y., Xu, C., Schuster, E., Luce, T. C., Ferron, J. R., Walker, M. L., and Humphreys, D. A., "Design and Simulation of Extremum-Seeking Open-Loop Optimal Control of Current Profile in the DIII-D Tokamak," *Plasma Physics and Controlled Fusion*, Vol. 50, No. 11, 2008, Paper 115001. doi:10.1088/0741-3335/50/11/115001
- [16] Binetti, P., Ariyur, K. B., Krstic, M., and Bernelli, F., "Formation Flight Optimization Using Extremum Seeking Feedback," *Journal of Guidance, Control, and Dynamics*, Vol. 26, No. 1, 2003, pp. 132–142. doi:10.2514/2.5024
- [17] Tan, Y., Moase, W. H., Manzie, C., Netic, D., and Mareels, I. M. Y., "Extremum Seeking from 1922 to 2010," *Proceedings of the 29th Chinese Control Conference*, IEEE Publ., Piscataway, NJ, 2010, pp. 14–26.
- [18] Sachs, G., "Optimization of Endurance Performance," *Progress in Aerospace Sciences*, Vol. 29, No. 2, 1992, pp. 165–191. doi:10.1016/0376-0421(92)90006-4
- [19] Sachs, G., Lenz, J., and Holzapfel, F., "Periodic Optimal Flight of Solar Aircraft with Unlimited Endurance Performance," *Applied Mathematical Sciences*, Vol. 4, No. 76, 2010, pp. 3761–3778.
- [20] Chen, R. H., and Speyer, J. L., "Improved Endurance of Optimal Periodic Flight," *Journal of Guidance, Control, and Dynamics*, Vol. 30, No. 4, 2007, pp. 1123–1133. doi:10.2514/1.27313
- [21] Chen, R. H., and Speyer, J. L., "Optimization and Mechanization of Periodic Flight," U.S. Patent Application Publication 2009/0177339 A1, 9 July 2009, p. 1.
- [22] Phillips, W. F., "Aircraft Performance," *Mechanics of Flight*, Wiley, Hoboken, NJ, 2004.
- [23] Roskam, J., and Lan, C. E., "Airplane Drag," *Airplane Aerodynamics and Performance*, DARcorporation, Lawrence, KS, 1997.
- [24] "Flying Qualities of Piloted Airplanes," MIL-SPEC MIL-F-8785C, 1980.
- [25] Khalil, H. K., *Nonlinear systems*, 3rd ed., Prentice–Hall, Upper Saddle River, NJ, 2002, p. 166.
- [26] Stankovic, M. S., and Stipanovic, D. M., "Extremum Seeking Under Stochastic Noise and Applications to Mobile Sensors," *Automatica*, Vol. 46, No. 8, 2010, pp. 1243–1251. doi:10.1016/j.automatica.2010.05.005
- [27] Moase, W. H., Manzie, C., and Brear, M. J., "Newton-Like Extremum-Seeking for the Control of Thermoacoustic Instability," *IEEE Transactions on Automatic Control*, Vol. 55, No. 9, Sept. 2010, pp. 2094–2105. doi:10.1109/TAC.2010.2042981